Article

The earliest human face of Western Europe

https://doi.org/10.1038/s41586-025-08681-0

Received: 11 June 2024

Accepted: 22 January 2025

Published online: 12 March 2025

Check for updates

Rosa Huguet[1,2,3]✉, Xosé Pedro Rodríguez-Álvarez[1,2]✉, María Martinón-Torres[4,5], Josep Vallverdú[1,2,3], Juan Manuel López-García[1,2], Marina Lozano[1,2], Marcos Terradillos-Bernal[6], Isabel Expósito[1,2], Andreu Ollé[1,2], Elena Santos[4,7,8], Palmira Saladié[1,2,3], Arturo de Lombera-Hermida[9,10], Elena Moreno-Ribas[1,2], Laura Martín-Francés[4,11], Ethel Allué[1,2], Carmen Núñez-Lahuerta[1,2,12,13], Jan van der Made[14], Julia Galán[12,15], Hugues-Alexandre Blain[1,2], Isabel Cáceres[1,2], Antonio Rodríguez-Hidalgo[1,16], Amèlia Bargalló[1,2], Marina Mosquera[1,2], Josep Maria Parés[4], Juan Marín[7,17], Antonio Pineda[1,18], David Lordkipanidze[19,20], Ann Margveslashvili[19,20,21], Juan Luis Arsuaga[7,22], Eudald Carbonell[1,2] & José María Bermúdez de Castro[4]✉

Who the first inhabitants of Western Europe were, what their physical characteristics were, and when and where they lived are some of the pending questions in the study of the settlement of Eurasia during the Early Pleistocene epoch. The available palaeoanthropological information from Western Europe is limited and confined to the Iberian Peninsula[1,2]. Here we present most of the midface of a hominin found at the TE7 level of the Sima del Elefante site (Sierra de Atapuerca, Spain), dated to between 1.4 million and 1.1 million years ago. This fossil (ATE7-1) represents the earliest human face of Western Europe identified thus far. Most of the morphological features of the midface of this hominin are primitive for the *Homo* clade and they do not display the modern-like aspect exhibited by *Homo antecessor* found at the neighbouring Gran Dolina site, also in the Sierra de Atapuerca, and dated to between 900,000 and 800,000 years ago[3]. Furthermore, ATE7-1 is more derived in the nasoalveolar region than the Dmanisi and other roughly contemporaneous hominins. On the basis of the available evidence, it is reasonable to assign the new human remains from TE7 level to *Homo* aff. *erectus*. From the archaeological, palaeontological and palaeoanthropological information obtained in the lower levels of the Sima del Elefante and Gran Dolina sites[4–8], we suggest a turnover in the human population in Europe at the end of the Early Pleistocene.

It is assumed that Eurasia was settled after the first expansion of hominins out of Africa, at least 1.8 million years ago (Ma), as attested by hominins recovered from the Dmanisi site in the Republic of Georgia[9,10]. In Western Europe, fossil evidence of the first human dispersal is limited to the Iberian Peninsula and dated between 1.4 Ma and 1.1 Ma (refs. 1,2,11). These hominins are represented by only a deciduous molar from Barranco León site (Orce, Spain)[2], and a phalanx and a mandibular fragment from Sima del Elefante site (Sierra de Atapuerca, Spain)[1,12], so their appearance is almost unknown and their taxonomic assignment is inconclusive[13]. With a younger chronology, the TD6 level of the Gran Dolina cave, also in the Sierra de Atapuerca, has provided human and faunal remains both with anthropogenic modifications and lithic industry[14–16]. The TD6 assemblage has been dated to the end of the Early Pleistocene[3,17,18] and the hominins assigned to the species *H. antecessor*[4]. One of the most striking features of this species is the modern-like morphology of the midface. This finding has prompted debate about the emergence of modern midfacial morphological features[19–21], necessarily limited by the paucity of facial remains in the Early Pleistocene fossil record of Eurasia. Here we present the midfacial fossil remains of a hominin found in the TE7 level of the Sima del Elefante cave site, dated to at least 1.1 Ma. This finding enables us to not only learn about the facial morphology of early Europeans, but also increase our knowledge of the evolutionary history of our ancestors in Europe and the roots of *H. antecessor*.

[1]Institut Català de Paleoecologia Humana i Evolució Social (IPHES-CERCA), Tarragona, Spain. [2]Departament d'Història i Història de l'Art, Universitat Rovira i Virgili (URV), Tarragona, Spain. [3]Unit associated to CSIC. Departamento de Paleobiología, Museo Nacional de Ciencias Naturales, Madrid, Spain. [4]Centro Nacional de Investigación sobre la Evolución Humana (CENIEH), Burgos, Spain. [5]Anthropology Department, University College London, London, UK. [6]Facultad de Humanidades y Ciencias Sociales, Universidad Internacional Isabel I de Castilla (Ui1), Burgos, Spain. [7]Centro Mixto UCM-ISCIII de Evolución y Comportamiento Humanos, Madrid, Spain. [8]Fundación Atapuerca, Ibeas de Juarros, Burgos, Spain. [9]Departamento de Historia, Universidad de Oviedo, Oviedo, Spain. [10]Centro de Investigación Interuniversitario das Paisaxes Atlánticas Culturais (CISPAC), Santiago de Compostela, Spain. [11]Department of Anatomy and Developmental Biology, Monash University, Melbourne, Victoria, Australia. [12]Aragosaurus-IUCA, Departamento de Ciencias de la Tierra, Facultad de Ciencias, Universidad de Zaragoza, Zaragoza, Spain. [13]Departamento de Geología, Facultad de Ciencia y Tecnología, Universidad del País Vasco/Euskal Herriko Unibertsitatea UPV/EHU, Leioa, Spain. [14]Departamento de Paleobiología, Museo Nacional de Ciencias Naturales-CSIC, Madrid, Spain. [15]Abteilung Messelforschung und Mammalogie, Senckenberg Forschungsinstitut und Naturmuseum, Frankfurt am Main, Germany. [16]Instituto de Arqueología-Mérida (CSIC-Junta de Extremadura), Mérida, Spain. [17]Departamento de Historia Facultad de Geografía e Historia, Universidad Nacional y Educación a Distancia (UNED), Madrid, Spain. [18]UMR 7194 HNHP (MNHN-CNRS-UPVD), Département Homme et Environnement, Muséum National d'Histoire Naturelle, Paris, France. [19]Georgian National Museum, Tiblisi, Georgia. [20]Ivane Javakshishvili Tiblisi State University, Tiblisi, Georgia. [21]The University of Georgia, Tbilisi, Georgia. [22]Departamento de Geodinámica, Estratigrafía y Paleontología, Universidad Complutense, Madrid, Spain. ✉e-mail: rhuguet@iphes.cat; xprodriguez@iphes.cat; josemaria.bermudezdecastro@cenieh.es

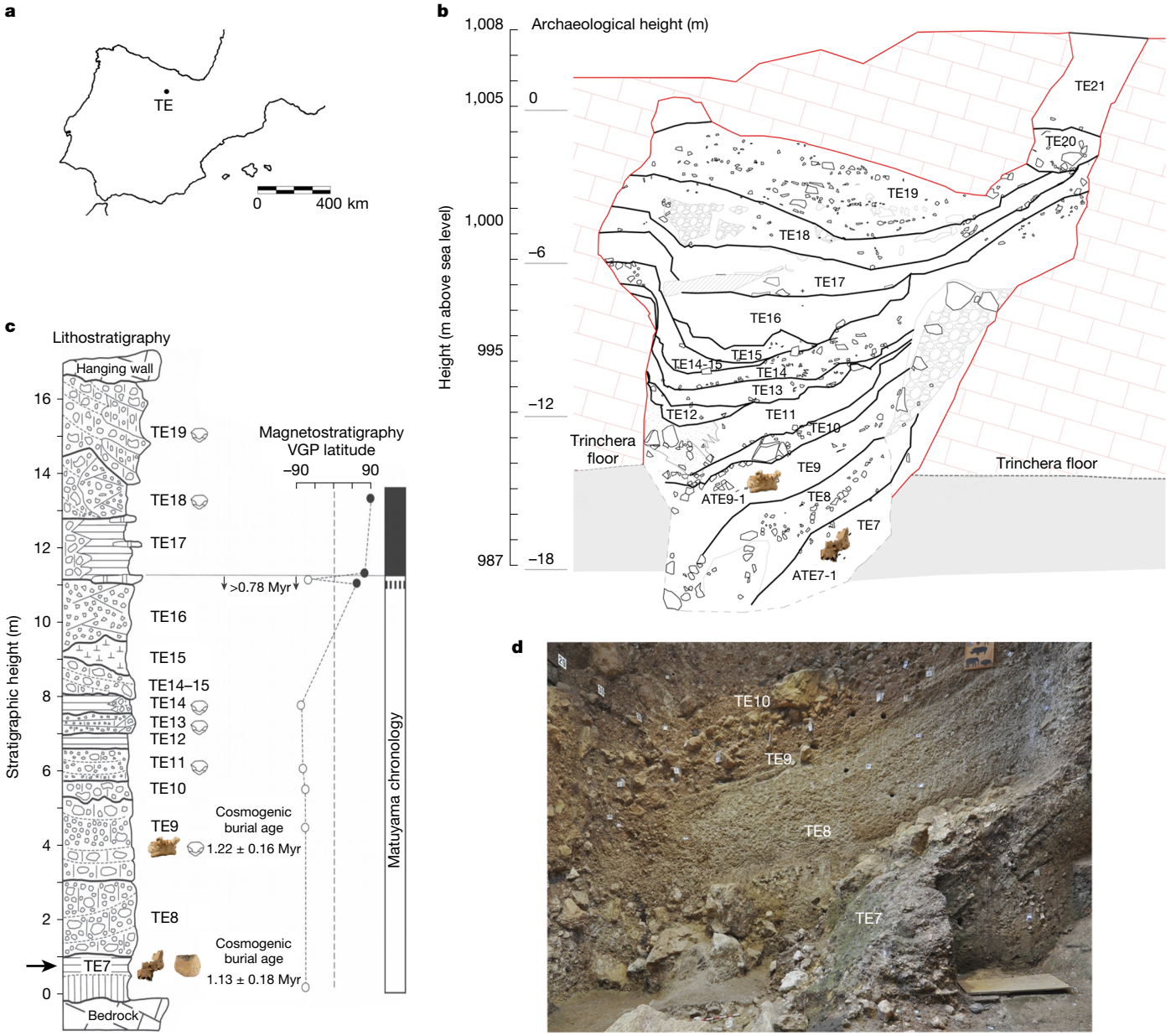

Fig. 1 | Stratigraphic section of Sima del Elefante, with the location of human remains recovered from levels TE9 and TE7. a, The location of Sima del Elefante in the Iberian Peninsula. **b**, Schematic of the stratigraphic section of Sima del Elefante with the location of the human remains (ATE9-1 and ATE7-1). **c**, Stratigraphic sequence of Sima del Elefante with cosmogenic burial ages[1], magnetostratigraphy and the location of the human fossils recovered in levels TE9 and TE7. **d**, View of the lower levels (TE7–TE10) on the Sima del Elefante North section. The stratigraphic sections of Sima del Elefante in **b** were drawn by R. Pérez-Martínez. For **c**, the figure was adapted from ref. 1.

The Sima del Elefante site

The Sima del Elefante site, located in Sierra de Atapuerca (Burgos, Spain), is a major cave with a visible sedimentary thickness of 25 m, filling a 15-m-wide conduit, divided into 16 lithostratigraphic units, TE7 to TE21, from bottom to top[22,23] (Fig. 1). Sima del Elefante presents the longest stratigraphic sequence within the archaeological record for the European Early Pleistocene. Along this sequence, we have recovered evidence of human presence, such as stone tools and bones with anthropogenic modifications[6,24,25], at almost all stratigraphic levels, whereas only the TE9 level had provided human remains[1,12,13] thus far. This level was dated on the basis of a combination of palaeomagnetism, cosmogenic nuclides and biostratigraphy to around 1.2 Ma (ref. 1). In 2022, the hominin fossil record from the Sima del Elefante site was significantly enriched with the discovery of a hominin midface (ATE7-1) in the TE7 level. ATE7-1 was found 2 m below the TE9 level in the stratigraphic succession. TE7 level is 1.5 m thick and stands out for its fissures, very undulating contacts and a dip of 40° to the north. Three sedimentary facies have been distinguished in TE7 level from top to bottom: yellowish-brown silts with very fine discontinuous laminations with horizontal fissures (paraclases/parallel joints); dark and very dark organic mineral red muds in thick laminations; and dark reddish muds with very fine to fine graded gravels stratified in fine to medium beds (Supplementary Information 1). From the biochronological point of view, the rodent assemblages that appear at TE7 and TE9 are the same and can be placed within the lower part of the Calabrian stage (Early Pleistocene), with an approximate age of 1.5–1.1 Ma (refs. 26,27).

Presently, the age at the TE7 and TE9 levels, based on radiometric and biochronological data is indistinguishable[1]. So far, we can confirm that

Fig. 2 | Specimen ATE7-1. Frontal view (**a**), lateral view (**b**) and occlusal view (**c**) of specimen ATE7-1 obtained at level TE7. Scale bars, 3 cm.

the age of the TE7 level is older than TE9 from their position within the stratigraphic sequence of Sima del Elefante (Fig. 1).

The human fossil ATE7-1

Specimen ATE7-1 consists of a substantial part of the maxilla and the zygomatic bone from the left side of an adult individual. The fossil was found in several fragments and was reconstructed by fitting the contact surfaces of the preserved fragments, as well as by virtual three-dimensional (3D) reconstruction techniques (Methods and Supplementary Information 2 and 3). This specimen preserves several fragments of the roots of the upper first molar (M^1), and the roots and part of the crown of the upper second molar (M^2). Both root systems fit in their corresponding alveoli (Fig. 2). The preserved part of the occlusal surface of the M^2 is worn, with dentine exposed on the lingual side.

The zygomatic bone is well preserved, except for the temporal process that is missing. The zygomaticofacial foramen is well visible. Below this foramen, the surface is highly roughened and there is a noticeable bulging at the origin of the zygomaticus and the levator labii superioris muscles' insertions. The frontal process is complete, preserving the serrated bony region where it articulates with the frontal bone. The frontal process is broad, measuring about 12.5 mm near the junction with the frontal bone. The orbital or anterosuperior border is intact, forming a part of the circumference of the orbit. The zygomatic border is irregular and rough, providing attachment to the masseter muscle. The inferior margin of the infraorbital plate (inferior zygomaxillary border) is straight (Extended Data Fig. 1). Although this border is not well preserved along its entire length, there are no clear signs of the presence of a zygomaxillary tubercle (Table 1, Figs. 2 and 3 and Extended Data Fig. 1). The zygomaxillary suture is partially preserved, and it can be followed either with the naked eye or by micro-computed tomography imaging of some sections of the maxillary process. A small fragment of the greater wing of the sphenoid articulates at the upper part of the posteromedial border of the zygomatic bone.

The maxilla preserves the zygomatic process, about 15 mm of the lateral nasal border, a part of the nasal sill, most of the alveolar process except the alveolar walls of the central incisor, the distal wall of the third molar and a part of the palatine process. The infraorbital plate is slightly sloped in an anteroinferior direction when viewed laterally (Table 1 and Extended Data Fig. 2). This region is completely flat from the

Table 1 | Comparison of some morphological features of the midface between ATE7-1 and hominins of the genus *Homo* from the Early Pleistocene

Feature	ATE7-1	*H. antecessor*[a]	Dmanisi[b]	*H. ergaster* (African *H. erectus*)[c]	Asian Early Pleistocene *H. erectus*[d]
Slope of the infraorbital plate	Anteroinferior	Posteroinferior	Anteroinferior	Anteroinferior	Anteroinferior
Inferior zygomaxillary border	Straight	Arced	Straight	Straight	Straight
Zygomaxillary tubercle	Absent	Present	Absent	Absent	Absent
Zygomatic root position	M^1	M^1	M^1/M^1–M^2	M^1/P^4–M^1	M^1/M^1–M^2
Maxillary flexion	Absent	Present	Absent	Absent	Absent
Canine fossa	Absent	Present	Absent	Absent	Absent
Sulcus maxillaris	Absent	Absent	Present	Present	Present
Malar tubercle	Present	Absent/present	Absent	Absent/present	Absent
Canine jugum	Absent	Absent	Present	Present	Present (weak)
Slope of the nasoalveolar clivus	Moderately sloped	Moderately sloped	Moderately sloped/ strongly sloped	Moderately sloped/ strongly sloped	Moderately sloped/ strongly sloped
Nasal floor topography	Discrete stepped	Discrete stepped	Discrete stepped/ continuous smooth	Continuous smooth	Continuous-smooth
Nasal lateral margin in lateral view	Vertical	Concave	Straight and slightly inclined forward	Vertical	Straight and slightly inclined forward

The Dmanisi hominins have been examined separately from the African hominins attributed to either *H. ergaster* or *H. erectus*, and from the Asian hominins assigned to *H. erectus*. P^4, upper second premolar.

[a]This sample is formed by the ATD6-19, ATD6-69 and ATD6-58 specimens. Although ATD6-69 belonged to an immature individual, further studies have confirmed that its morphology would not have changed if it had reached the adult stage[19,20].

[b]This sample is formed by the D2282, D2700 and D4500 specimens. D2700 also belonged to an immature individual and its facial dimensions may have increased in size. However, its morphology would probably not have changed in the adult state.

[c]This sample is formed by the KNM-ER-3733 and KNM-WT-15000 specimens.

[d]This sample is formed by the Sangiran 4, Sangiran 17 and Gonwangling specimens.

maxillary zygomatic process to the lateral nasal border and no flexion of the infraorbital plate is observed at the level of the lateral nasal wall (Table 1 and Extended Data Fig. 3). The zygomatic root is centred over the level of the M^1 roots. There is no evidence of either a canine fossa[28] or a sulcus maxillaris[29] (Table 1). Owing to the fragmentary state of ATE7-1, the infraorbital foramen is not preserved. However, the infraorbital groove is observed in the internal part of the maxilla. The lowermost facial (or nasoalveolar) contour is flat, slightly sloped and smooth, and the canine jugum is barely marked (Extended Data Fig. 4). Only a small part of the nasoalveolar clivus is preserved. Although most of the alveolar walls of the incisors are missing, the length of the clivus can be estimated to be small (<20 mm) compared with that obtained in other Early Pleistocene specimens from Africa and Eurasia[30,31]. Most of the premaxilla (os incisivum) is missing, and it is not possible to examine either the incisive canal or the corresponding part of the nasal floor. The palatine process of the maxilla is incomplete, and the palatine bone is missing. The floor of the hard palate is rough and two palatine spines are observed at the posterior end of the palatine process (Supplementary Information 2).

The estimated buccolingual dimension of the preserved part of the crown of the M^2 is about 14 mm. The mesial interproximal wear facet is very marked. On the mesial side of the M^2, there is a buccolingually elongated interproximal groove located below the cementoenamel junction. The groove runs along the entire mesial surface and shows a semi-circular cross-section with softened and polished walls. The bottom of the groove shows fine and parallel microscratches that are buccolingually oriented. The width of the groove is between 2 mm and 3.7 mm and the deepest part of the groove measures 675.51 µm. The interproximal groove is an anomalous wear and should be caused by pulling some type of narrow, long and hard object between adjacent molars, probably a toothpick[32]. The roots are robust, stout and column-like, and they do not narrow towards the tip. In both the M^1 and the M^2, the two buccal roots are parallel and converge in the apical third, whereas the lingual root diverges strongly from the buccal ones (Supplementary Information 2). No signs of taurodontism are present. Each root has one canal, except for the mesiobuccal one that presents two separate canals, one mesiobuccal and one mesiodistal, that bifurcate at the apical third. The heavily built and column-like roots together with the highly divergent lingual radical are typically found in African and East Asian Early Pleistocene and Asian Middle Pleistocene specimens and are different from the more gracile roots of the European Early and Middle Pleistocene specimens[33].

The nasal floor configuration of ATE7-1 is sloped, according to the Franciscus' classification[34]. Following the terminology proposed previously[35], we can observe at least the anterior nasal crest, the subnasal fossa, the middle nasal crest and the intranasal fossa. This nasal floor topography is stepped-discrete in the terminology of McCollum[36] (Table 1). It is noteworthy that, in lateral view, the lateral nasal border is almost straight (it barely describes a very smooth curve) from the nasal sill up to the point where the bone was broken post mortem (Fig. 2 and Extended Data Fig. 5). The length of this section is approximately 17 mm. Thus, the lateral nasal margin does not describe the pronounced curve that appears when the nasal margin meets the outermost point of an anteriorly projected nasal bone (Extended Data Figs. 2, 4 and 5). Considering this feature and that ATE7-1 lacks flexion of the infraorbital plate in the region of the lateral nasal wall, we can speculate that the hominin from the ATE7 level of the Sima del Elefante cave may not have had a projected nose (Extended Data Figs. 3 and 5).

Archaeopalaeontological record

Three lithic artefacts on siliceous materials were recovered from the TE7 level (Supplementary Information 4). A small quartz flake was recovered in 2021, whereas a cobble tool on quartz and a small chert flake were recovered in 2023. The quartz flake, probably a knapping debris, measures 8 × 11 × 3 mm and has a remnant of cortex on its dorsal face, but there is no cortex in the striking platform. Three small removals on the dorsal face highlight the recurrence of the knapping sequences. The cobble tool measures 84 × 78 × 43 mm and was shaped just through two unifacial and unidirectional removals. The purpose may have been to shape a convex middle angled edge (75°), slightly incurvated in profile.

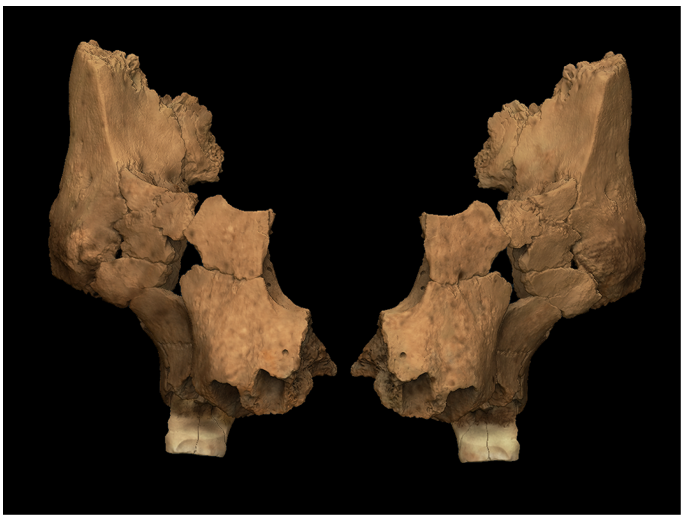

Fig. 3 | Frontal view of the virtual reconstruction of ATE7-1. The right side was mirror imaged from the preserved left one. Details of the reconstruction are provided in the Methods.

Preliminary use-wear and residue analysis points to its involvement in bone breakage activities (Supplementary Information 4.3.3). The only chert flake measures 16 × 16 × 4 mm and has no cortical remains. On its dorsal side, there are two negatives of previous extractions. The raw materials (quartz and chert) were probably obtained in the vicinity of the site, less than 2 km away (Fig. 4).

Moreover, several limestone objects were found at the TE7 level, not in all cases of irrefutable anthropic origin. Preliminary analysis shows that 12 of these limestone objects have characteristics that are consistent with the anthropic knapping already documented in similar objects from level TE9[37] (Supplementary Information 4.3.2).

The faunal assemblage from TE7 comprises about 6,000 fossil remains, where Aves, Rodentia and Ungulata are the taxonomic groups with a higher number of specimens. Most of the mammals documented in the assemblage are represented by long bones, although some skeletons of *Sus* sp. and Aves have been recovered almost complete and in anatomical connection, which would indicate that these animals skeletonized inside the cavity. Anthropogenic modifications on faunal remains are exceptional: a rib of a small-sized animal shows, on its dorsal side, defleshing cut marks (Fig. 4 and Supplementary Information 5).

The palaeontological and palaeobotanical data are indicative of the environmental conditions during the formation of the TE7 level. These data suggest an open humid forest landscape with trees, shrubs and water courses in the vicinity of the cave. From a faunistic point of view, this environment is suggested mainly by the relative abundance of water vole species such as *Arvicola jacobea*, the mouse species *Apodemus* sp. and *Castillomys rivas*, as well as the slow worm *Anguis fragilis*, *Macaca* cf. *sylvanus* and a few ungulates, mostly *Bison schoetensacki*, *Eucladoceros giulii* and *Hipoppotamus georgicus* (Supplementary Information 6). The anthracological and palynological results from TE7 are not statistically representative but provide information on the occasional presence of some taxa. The plant assemblage identified corresponds to a Mediterranean-type environment, including areas of arboreal vegetation (*Pinus* sp., cf. *Juniperus*, *Quercus ilex coccifera* type, *Quercus* sp. deciduous and *Prunus* sp.) and open areas with proliferation of plants associated with meadows. We also documented the presence of hazel (*Corylus*), a mesophilous tree that can grow among other deciduous taxa in certain humidity contexts, or sedges (Cyperaceae), which must have been abundant in wet soils, such as those near rivers or water sources (Supplementary Information 7). All of these are indicative of moisture conditions, possibly at the regional scale, in agreement with the small vertebrate data, particularly the relative abundance of *A. fragilis*.

The palaeontological data, mainly from small-vertebrate proxies, point to a reduction in the woodland and increasing of the open dry areas from TE7 to TE9 (ref. 38), always within of a mild climate condition[39] (Supplementary Information 6 and 7). However, as already mentioned above, the rodent assemblages recovered at both levels suggest that they are chronologically close. For this reason, it seems reasonable to propose that the human remains obtained at levels TE9 (mandible ATE9-1) and TE7 (maxilla ATE7-1) could belong to the same species, which lived in the Sierra de Atapuerca at least 1.1 Ma ago.

ATE7-1 in the first settlement of Europe

Important differences are observed between ATE7-1 and *H. antecessor* (Table 1). In ATD6-69, the infraorbital plate slopes down and backwards, like in *Homo sapiens*, whereas, in ATE7-1, this region is slightly sloped in anteroinferior direction (Extended Data Fig. 2). *H. antecessor* shows an arced zygomaxillary border and a marked zygomaxillary tubercle, whereas this tubercle is absent in ATE7-1, and the border is straight (Extended Data Figs. 5 and 6). In a transverse section, *H. antecessor* shows a maxillary flexion, from the coronal orientation of the infraorbital plate to a more sagittal position of the lateral nasal wall[30]. This flexion is absent in ATE7-1, which also lacks a canine fossa. Finally, the nasal lateral margin of ATE7-1 is vertical, whereas it is clearly concave in ATD6-69 (Extended Data Fig. 5). Thus, ATE7-1 does not exhibit the modern-like midface of *H. antecessor*, and we can confidently conclude that this specimen belonged to a different species than that recovered from the TD6 level of the Gran Dolina cave site.

ATE7-1 differs from the Dmanisi hominins in the absence of a pillar-like and laterally swollen canine jugum and a sulcus maxillaris, as well as in the absence of a well-developed and sloped subnasal clivus. The zygomatic root has a more backward position in D4500 (M^1–M^2). Regarding *Homo ergaster* (African *H. erectus*), the main differences compared with ATE7-1 also lie in the presence of a marked canine jugum and sulcus maxillaris, a moderately to strongly sloped clivus and a smooth nasal topography in the African specimens (Table 1). Moreover, the zygomatic root has a more advanced position in *H. ergaster*. A moderate canine jugum is also present in Asian *H. erectus*. The slope of the clivus is very marked in Sangiran 4, and the nasal topography is smooth. The absence of a canine jugum and a moderately sloped nasoalveolar clivus seems to be derived features of ATE7-1 for the *Homo* clade. The maxillary breadth of ATE7-1 hominin is relatively small, similar to that of D2280 and D2700 and below KNM-ER-3733 and Sangiran 17 values (Supplementary Information 2 and Supplementary Table 2.1). As the zygion is not preserved, it is not possible to estimate the bizygomatic breadth of ATE7-1. However, in the frontal view, ATE7-1 stands out as a very narrow in contrast to the broad midfaces of African and Asian *H. erectus* specimens, where the robust zygomatic bones are strongly projected laterally (Extended Data Fig. 6).

For some authors[40], the metric and morphological variability of specimens such as KNM-ER-3733 or KNM-WT-15000 is indistinguishable from that of Asian *H. erectus*. Furthermore, the variability of Dmanisi hominins could also be included in the hypodigm of *H. erectus*[30,31]. We found similarities but also some notable differences between ATE7-1 and the fossils that are generally referred to as *H. erectus* sensu lato. Even if ATE9-1 and ATE7-1 were considered to be members of the same species, the evidence is still limited for a robust conclusion on their taxonomic position. In awareness of the similarities but also the differences, and pending further evidence from other contemporary European sites, we propose the provisional assignment of ATE7-1 to *H.* aff. *erectus*.

The fossil record recovered at Sima del Elefante strengthens the evidence for the first settlement of Western Europe around 1.4 Ma and opens up scenarios for discussion. Most of the European sites with chronologies between 1.4 Ma and 1.1 Ma, such as Fuente-Nueva-3 (ref. 41), Barranco León[2], Le Vallonnet[42], Pont-de-Lavaud[43], Kocabas[44] or Pirro

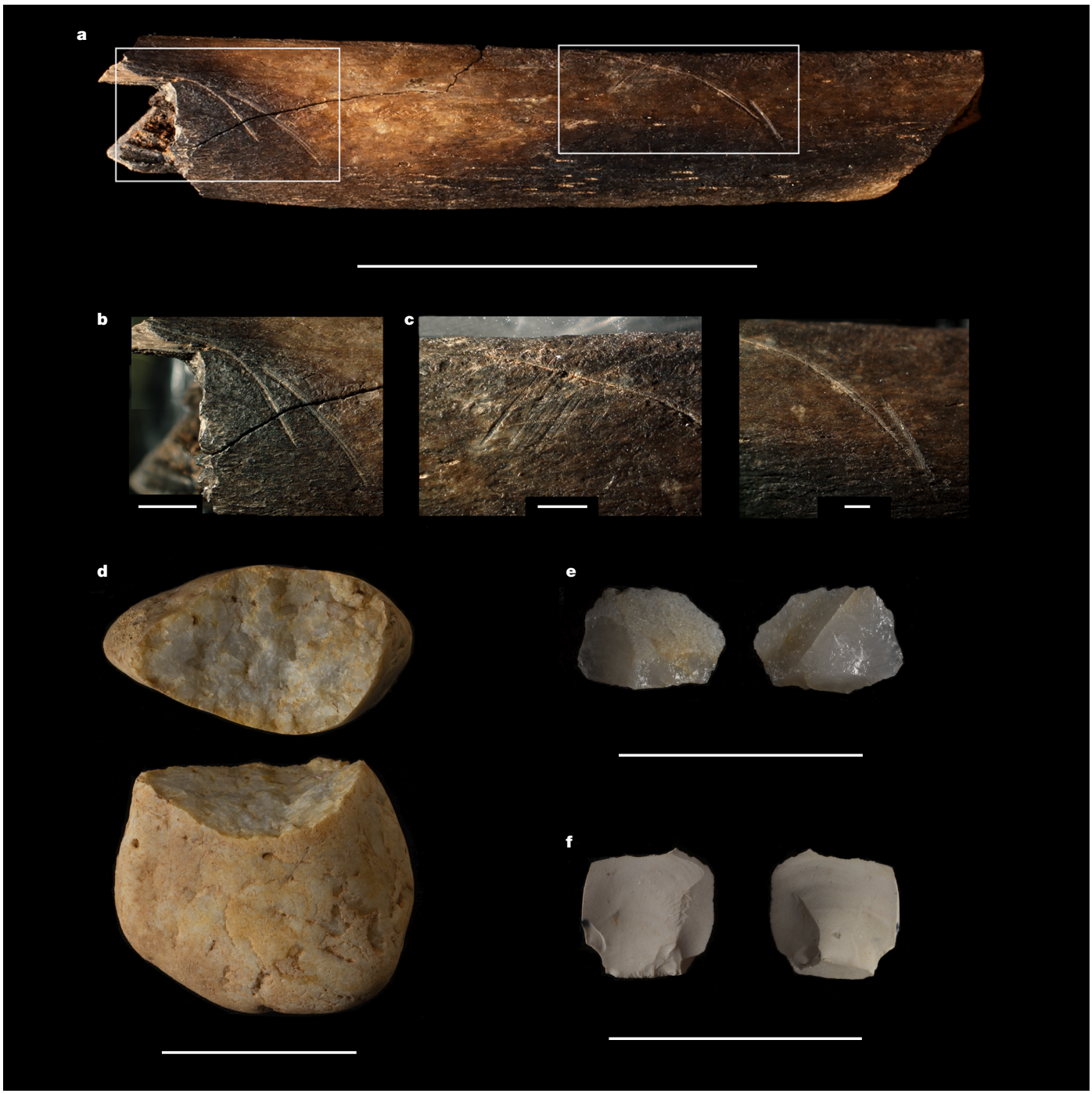

Fig. 4 | Faunal remains and lithic artefacts from level TE7 of Sima del Elefante. a, Rib of a small animal (dorsal side view) with anthropogenic modifications. **b**, Cut marks interrupted by a fissure. **c**, Cut marks interrupted by abrasion striations (trampling) (left), and detail of the cut mark (right) (Supplementary Information 5). **d**, Quartz cobble with unifacial removals. **e**, Quartz flake. **f**, Flake made with Cretaceous chert. Scale bars, 2 cm (**a** and **e**), 2 mm (**b**), 1 mm (**c**, left), 800 μm (**c**, right), 5 cm (**d**) and 3 cm (**f**).

Nord[45,46], are located in the south of the continent, around the Mediterranean basin[8]. The Kocabas skull[44], interpreted as different to the Dmanisi specimens, could be additional evidence of a hominin expansion into Europe different to the one documented at the Georgian site. However, the recent publication of the Korolevo 1 site[47], to the east of the European continent suggests that these early human groups were able of inhabiting higher latitudes, albeit perhaps discontinuously. Moreover, it reinforces the hypothesis that the first settlement occurred from Eastern to Western Europe at least 1.4 Ma.

It was documented[5] that the terrestrial small mammal assemblages found at the Early Pleistocene levels (TD3/4-TD7) of the Gran Dolina site, dated to 0.9–0.78 Ma[7], show a different composition than that found at the Early Pleistocene levels (TE7–TE14) of the Sima del Elefante site. Only five out of a total of 36 taxa are common to both sites, suggesting a chronological gap between them[5]. In this context, some authors[48] have suggested a depopulation of Europe during MIS34, due to the extreme climatic conditions inferred in the analysis of a deep-sea core on the Portuguese margin and that would support a discontinuity between the Gran Dolina-TD6 and the Sima del Elefante hominin populations. Previous palaeoenvironmental data obtained through different proxies[49] did not reflect such a severe worsening of the conditions from TE7 to TD6 that could be related to a total depopulation of the Iberian Peninsula,

but they could still have favoured a demographic decline in the *H.* aff. *erectus* population. This scenario would be in accordance with the severe human bottleneck around 900,000 years ago proposed previously[50].

Here we present strong evidence to suggest that Western Europe was populated by at least two different *Homo* species during the Early Pleistocene: *H.* aff. *erectus*, represented at TE7 and possibly TE9; and, later, *H. antecessor*. Scenarios for this turnover are various, including the possibility that a residual population of *H.* aff. *erectus* coincided for a short time with *H. antecessor*, if climatic conditions at Sierra de Atapuerca were not as dramatic as suggested previously[48]. However, we cannot rule out the complete disappearance of the species represented at the lower levels of the Sima del Elefante before the arrival of *H. antecessor*. New discoveries at the Sima del Elefante site and other European sites will allow the testing of these hypotheses and making a more precise taxonomic assignment of human remains from Sima del Elefante. Future research will provide further insights into the origin and dynamics of the initial settlement of Western Europe.

Online content

Any methods, additional references, Nature Portfolio reporting summaries, source data, extended data, supplementary information, acknowledgements, peer review information; details of author contributions and competing interests; and statements of data and code availability are available at https://doi.org/10.1038/s41586-025-08681-0.

1. Carbonell, E. et al. The first hominin of Europe. *Nature* **452**, 465–469 (2008).
2. Toro-Moyano, I. et al. The oldest human fossil in Europe, from Orce (Spain). *J. Hum. Evol.* **65**, 1–9 (2013).
3. Duval, M. et al. The first direct ESR dating of a hominin tooth from Atapuerca Gran Dolina TD-6 (Spain) supports the antiquity of *Homo antecessor*. *Quat. Geochronol.* **47**, 120–137 (2018).
4. Bermúdez de Castro, J. M. et al. A hominid from the Lower Pleistocene of Atapuerca, Spain: possible ancestor to Neandertals and modern humans. *Science* **276**, 1392–1395 (1997).
5. Cuenca-Bescós, G. et al. Comparing two different Early Pleistocene microfaunal sequences from the caves of Atapuerca, Sima del Elefante and Gran Dolina (Spain): biochronological implications and significance of the Jaramillo subchron. *Quat. Int.* **389**, 148–158 (2015).
6. Huguet, R. et al. Successful subsistence strategies of the first humans in south-western Europe. *Quat. Int.* **295**, 168–182 (2013).
7. Parés, J. M. et al. Chronology of the cave interior sediments at Gran Dolina archaeological site, Atapuerca (Spain). *Quat. Sci. Rev.* **186**, 1–16 (2018).
8. Carbonell, E., Rodríguez-Álvarez, X. P., Parés, J. M., Huguet, R. & Rosell, J. The earliest human occupation of Atapuerca in the European context. *Anthropologie* **128**, 103233 (2024).
9. Gabunia, L. et al. Earliest pleistocene hominid cranial remains from Dmanisi, Republic of Georgia: taxonomy, geological setting, and age. *Science* **288**, 1019–1025 (2000).
10. Garcia, T. et al. Earliest human remains in Eurasia: new $^{40}Ar/^{39}Ar$ dating of the Dmanisi hominid-bearing levels, Georgia. *Quat. Geochronol.* **5**, 443–451 (2010).
11. Oms, O. et al. Early human occupation of Western Europe: paleomagnetic dates for two paleolithic sites in Spain. *Proc. Natl Acad. Sci. USA* **97**, 10666–10670 (2000).
12. Lorenzo, C. et al. Early Pleistocene human hand phalanx from the Sima del Elefante (TE) cave site in Sierra de Atapuerca (Spain). *J. Hum. Evol.* **78**, 114–121 (2015).
13. Bermúdez De Castro, J. M. et al. Early Pleistocene human mandible from Sima del Elefante (TE) cave site in Sierra de Atapuerca (Spain): a comparative morphological study. *J. Hum. Evol.* **61**, 12–25 (2011).
14. Fernández-Jalvo, Y., Díez, J. C., Bermúdez de Castro, J. M., Carbonell, E. & Arsuaga, J. L. Evidence of early cannibalism. *Science* **271**, 277–278 (1996).
15. Díez, J. C., Fernández-Jalvo, Y., Rosell, J. & Cáceres, I. Zooarchaeology and taphonomy of Aurora Stratum (Gran Dolina, Sierra de Atapuerca, Spain). *J. Hum. Evol.* **37**, 623–652 (1999).
16. Saladié, P. et al. Dragged, lagged, or undisturbed: reassessing the autochthony of the hominin-bearing assemblages at Gran Dolina (Atapuerca, Spain). *Archaeol. Anthropol. Sci.* **13**, 65 (2021).
17. Parés, J. M. & Pérez-González, A. Paleomagnetic age for hominid fossils at Atapuerca archaeological site, Spain. *Science* **269**, 830–832 (1995).
18. Falguères, C. et al. Earliest humans in Europe: the age of TD6 Gran Dolina, Atapuerca, Spain. *J. Hum. Evol.* **37**, 343–352 (1999).
19. Freidline, S. E., Gunz, P., Harvati, K. & Hublin, J.-J. Evaluating developmental shape changes in *Homo antecessor* subadult facial morphology. *J. Hum. Evol.* **65**, 404–423 (2013).
20. Lacruz, R. S. et al. Facial morphogenesis of the earliest Europeans. *PLoS ONE* **8**, e65199 (2013).
21. Lacruz, R. S. et al. The evolutionary history of the human face. *Nat. Ecol. Evol.* **3**, 726–736 (2019).
22. Rosas, A. et al. Le gisement pléistocène de la «Sima del Elefante å (Sierra de Atapuerca, Espagne). *Anthropologie* **105**, 301–312 (2001).
23. Rosas, A. et al. The "Sima del Elefante" cave site at Atapuerca (Spain). *Estud. Geol.* **62**, 327–348 (2006).
24. Huguet, R. et al. Level TE9c of Sima del Elefante (Sierra de Atapuerca, Spain): a comprehensive approach. *Quat. Int.* **433**, 278–295 (2017).
25. De Lombera-Hermida, A. et al. The lithic industry of Sima del Elefante (Atapuerca, Burgos, Spain) in the context of Early and Middle Pleistocene technology in Europe. *J. Hum. Evol.* **82**, 95–106 (2015).
26. Cuenca-Bescós, G. et al. The small mammals of Sima del Elefante (Atapuerca, Spain) and the first entrance of *Homo* in Western Europe. *Quat. Int.* **295**, 28–35 (2013).
27. Cuenca-Bescós, G. et al. Updated Atapuerca biostratigraphy: small-mammal distribution and its implications for the biochronology of the Quaternary in Spain. *C. R. Palevol* **15**, 621–634 (2016).
28. Maureille, B. *La Face Chez* Homo erectus *et* Homo sapiens: *Recherche Sur La Variabilite Morphologique et Métrique*. PhD thesis, Univ. Bourdeux I (1994).
29. Weidenreich, F. The skull of *Sinanthropus pekinensis*: a comparative study. *Paleontol. Sin. N. D* **10**, 1–484 (1943).
30. Rightmire, G. P., Lordkipanidze, D. & Vekua, A. Anatomical descriptions, comparative studies and evolutionary significance of the hominin skulls from Dmanisi, Republic of Georgia. *J. Hum. Evol.* **50**, 115–141 (2006).
31. Rightmire, G. P., Ponce De León, M. S., Lordkipanidze, D., Margvelashvili, A. & Zollikofer, C. P. E. Skull 5 from Dmanisi: descriptive anatomy, comparative studies, and evolutionary significance. *J. Hum. Evol.* **104**, 50–79 (2017).
32. Ungar, P. S., Grine, F. E., Teaford, M. F. & Pérez-Pérez, A. A review of interproximal wear grooves on fossil hominin teeth with new evidence from Olduvai Gorge. *Arch. Oral Biol.* **46**, 285–292 (2001).
33. Xing, S., Martinón-Torres, M. & Bermúdez de Castro, J. M. The fossil teeth of the Peking Man. *Sci. Rep.* **8**, 2066 (2018).
34. Franciscus, R. G. Internal nasal floor configuration in *Homo* with special reference to the evolution of Neandertal facial form. *J. Hum. Evol.* **44**, 701–729 (2003).
35. Schwartz, J. H., Pantoja-Pérez, A. & Arsuaga, J. L. The nasal region of the 417 ka Sima de los Huesos (Sierra de Atapuerca, Spain) Hominin: new terminology and implications for later human evolution. *Anat. Rec.* **305**, 1991–2029 (2022).
36. McCollum, M. A. Subnasal morphological variation in fossil hominids: a reassessment based on new observations and recent developmental findings. *Am. J. Phys. Anthropol.* **112**, 275–283 (2000).
37. Terradillos-Bernal, M., Zorrilla-Revilla, G. & Rodríguez-Álvarez, X.-P. To be or not to be a lithic tool: analysing the limestone pieces of Sima del Elefante (Sierra de Atapuerca, northern Spain). *Archaeol. Anthropol. Sci.* **14**, 189 (2022).
38. Nuñez-Lahuerta, C., Cuenca-Bescós, G. & Huguet, R. First report on the birds (Aves) from level TE7 of Sima del Elefante (Early Pleistocene) of Atapuerca (Spain). *Quat. Int.* **421**, 12–22 (2016).
39. Galán, J., Cuenca-Bescós, G. & López-García, J. M. The fossil bat assemblage of Sima del Elefante Lower Red Unit (Atapuerca, Spain): first results and contribution to the palaeoenvironmental approach to the site. *C. R. Palevol* **15**, 647–657 (2016).
40. Rightmire, G. P. Evidence from facial morphology for similarity of Asian and African representatives of *Homo erectus*. *Am. J. Phys. Anthropol.* **106**, 61–85 (1998).
41. Barsky, D. et al. The significance of subtlety: contrasting lithic raw materials procurement and use patterns at the Oldowan sites of Barranco León and Fuente Nueva 3 (Orce, Andalusia, Spain). *Front. Earth Sci.* **10**, 893776 (2022).
42. Cauche, D. The Vallonnet cave on the northern Mediterranean border: a record of one of the oldest human presences in Europe. *Anthropologie* **126**, 102974 (2022).
43. Despriée, J. et al. The 1-million-year-old quartz assemblage from Pont-de-Lavaud (Centre, France) in the European context. *J. Quat. Sci.* **33**, 639–661 (2018).
44. Vialet, A., Prat, S., Wils, P. & Cihat Alçiçek, M. The Kocabaş hominin (Denizli Basin, Turkey) at the crossroads of Eurasia: new insights from morphometric and cladistic analyses. *C. R. Palevol* **17**, 17–32 (2018).
45. Arzarello, M., De Weyer, L. & Peretto, C. The first European peopling and the Italian case: peculiarities and "opportunism". *Quat. Int.* **393**, 41–50 (2016).
46. Duval, M. et al. Re-examining the earliest evidence of human presence in western Europe: new dating results from Pirro Nord (Italy). *Quat. Geochronol.* **82**, 101519 (2024).
47. Garba, R. et al. East-to-west human dispersal into Europe 1.4 million years ago. *Nature* **627**, 805–810 (2024).
48. Margari, V. et al. Extreme glacial cooling likely led to hominin depopulation of Europe in the Early Pleistocene. *Science* **381**, 693–699 (2023).
49. Rodríguez, J. et al. One million years of cultural evolution in a stable environment at Atapuerca (Burgos, Spain). *Quat. Sci. Rev.* **30**, 1396–1412 (2011).
50. Hu, W. et al. Genomic inference of a severe human bottleneck during the Early to Middle Pleistocene transition. *Science* **381**, 979–984 (2023).

Methods

This paper is the result of the interdisciplinary work carried out by the Atapuerca Research Team. The interdisciplinary approach starts with fieldwork, the basis for the archaeological and palaeoanthropological studies. Sima del Elefante site have been studied following systematic excavation, all items recovered were registered in a three-dimensions coordinate system and placed in stratigraphic context.

In the following text, we present the methods related to the palaeoanthropological study of fossil ATE7-1. The full methods and any associated references are available in the Supplementary information.

Morphological features

We used the most significant morphological characters of the midface to compare the specimen ATE7-1 with other approximately contemporary specimens of the genus *Homo*. In particular and for taxonomic purposes, we considered that this comparison should focus on *H. antecessor*, because this taxon was found at a site about 200 m away from the Sima del Elefante cave site, as well as on specimens from the Dmanisi site (Republic of Georgia); African specimens attributed by some to *H. ergaster* (African *H. erectus*); and Asian specimens from the Early Pleistocene. For these comparisons, we looked at the originals of Dmanisi and *H. antecessor* specimens and some good quality casts and 3D models, and consulted specialized references[30,31,40]. A glossary of the terms used in Table 1 is provided in Supplementary Information 2.

Micro-computed tomography

The morphology of the face and the teeth are described on the basis of the analysis of the original fossils and/or virtual reconstruction after micro-computed tomography scanning. ATE7-1 facial and dental morphology was compared to a wide sample of Early and Middle Pleistocene fossils from Africa, Asia and Europe, as well as to Neanderthals and modern humans.

The original fossil was found in several fragments (Supplementary Information 3) that were individually scanned at the Microscopy and Micro-computed Tomography Laboratory of the National Research Center on Human Evolution-Unique Scientific and Technical Infrastructure (CENIEH–ICTS, Burgos) using the Phoenix v|tome|x s (GE Measurement & Control) system. ATE 7-1 was scanned with an isotropic voxel size ranging from 22 to 40 µA (100–125 kV and 240–270 µA, with a 0.2-mm Cu filter) and an integration time of 333–600 ms. The segmentation of the dental tissues allowed the reconstruction of the radicular canals (Supplementary Information 2 and Supplementary Fig. 2.1). The observation of the morphology of the groove on the mesial surface of the upper second molar was performed using a HIROX KH-8700 3D digital microscope under a range of ×35 to ×100 magnifications using a ring light of Social Evolution and Human Paleoecology Institute (IPHES-CERCA, Tarragona). The bottom and morphology of the groove was also analysed using a Sensofar S Neox confocal microscope at ×5 and ×20 magnifications.

Virtual reconstruction

Segmentation of the micro-computed tomography data was performed in Avizo (Visualization Sciences Group) and Mimics (Materialise). Parallel to the physical reconstruction of the fossil (Supplementary Information 3) the face was virtually reconstructed by associating the individual segmented surfaces of each scan, consisting of two maxillary fragments, a nearly complete left zygomatic bone and a sphenoid fragment bone. Through the examination of the original fossils and by using Mimics and Meshlab, the fitting and alignment of each fragment with each other was explored considering anatomical reference and contact points. The final adjustment of the four fragments was obtained by applying the global registration tool, which maximizes the overlap of the contact areas of the different fragments.

We next used several Early and Middle Pleistocene hominins and anatomically recent modern human (RMH) as a reference to orientate the left maxillary and zygomatic bones (Supplementary Information 2 and Supplementary Table 2.1) and to define a sagittal plane for ATE7-1. As a large portion of the maxillary bone, dental arcade, the occlusal plane and orbital floor is preserved, the possibilities of the orientation were limited to no more than 2–3 mm in the following ways: broadening the palate; increasing the facial height; increasing the orbital height; or rotating the zygomatic bones anteriorly or posteriorly in a parasagittal direction. For each reconstruction, the ATE-1 preserved fragments were mirror imaged along the sagittal plane of ATE7-1 and merged to form one surface model. Finally, as the suture of the palatine process was missing, the distance between the left and right palatal halves was estimated by measuring as a reference the mesiodistal distance of the incisor area, as well as the distance between left and right upper second molars (that is, the proportions of the dental arch) in several *Homo* specimens. Then, the mirrored ATE7-1 specimen was adjusted to fit this proportion (Supplementary Information 2 and Supplementary Fig. 2.2).

Reporting summary

Further information on research design is available in the Nature Portfolio Reporting Summary linked to this article.

Data availability

Correspondence and requests data/materials should be addressed to R.H., X.P.R.-Á., J.M.B.d.C. and M.M.-T.

Acknowledgements We acknowledge all of the members of the Atapuerca research team involved in the recovery and study of the archaeological and palaeontological record from Sima del Elefante site. The research of the Atapuerca sites is founding by the Spanish Ministry of Science and Innovation and European Regional Development Fund "ERDF A way of making Europe" (projects PID2021-122355NB-C31, PID2021-122355NB-C32, PID2021-22355NB-C33). Fieldwork at Sima del Elefante is supported by the Junta de Castilla y León and the Fundación Atapuerca. The Institut Català de Paleoecologia Humana i Evolució Social (IPHES-CERCA) has received financial support from the Spanish Ministry of Science and Innovation through the María de Maeztu program for Units of Excellence (CEX2019-000945-M). We acknowledge support from the Catalan Government (AGAUR, projects 2021-SGR-01237, 2021-SGR-01238 and 2021-SGR-01239) and Universitat Rovira i Virgili (2023PFR-URV-01237, 2023PFR-URV-01238 and 2023PFR-URV-01239). M.M.-T. receives funding from The Leakey Foundation through the personal support of D. Crook. Part of the hominin analyses were carried out at the laboratories of the CENIEH-ICTS with the support of the CENIEH staff. The research of J.M.L.-G. and H.-A.B. was funded by the Spanish Ministry of Science and Innovation and European Regional Development Fund (project PID2021-122533NB-I00). E.S. received funding from Fundación Atapuerca. C.N.-L. was supported by a Juan de la Cierva formation contract (FJC2020-044561-I; MCIN cofinanced by the NextGeneration EU/PRTR). L.M.-F. is supported by Horizon Program-Marie Sklodowska-Curie Actions of the EU Ninth programme (2021–2027) under the HORIZON-MSCA-2021-PF-01-Project: 101060482 and MCIN/AEI/10.13039/501100011033 and "ERDF A way of making Europe". J.G. is the beneficiary of a Postdoctoral Fellowship from the Alexander von Humboldt Foundation (ESP-1235332-HFST-P). J.v.d.M. benefited from grant Synthesys AT-TAF-3663. The research of A.R.-H. is supported by the grant RYC2022-037802-I funded by MCIN/AEI/10.13039/501100011033 and by the FSE invests in your future. A.B. was supported by a Juan de la Cierva—Incorporación contract IJC2019-041546-I and by the grant RYC2022-037783-I. A.P. is supported by the LATEUROPE project (ERC Consolidator Grant ID101052653). A.M. acknowledges the Shota Rustaveli Georgian National Science Foundation (grant YS-21-1595). All of the photographs of the archaeological and palaeontological remains of Sima del Elefante were taken by M. D. Guillén (IPHES-CERCA). The stratigraphic sections of Sima del Elefante were drawn by R. Pérez-Martínez. We thank G. Zorrilla-Revilla and P. Mateo-Lomba for assistance on the microscopy analysis of archaeological remains.

Author contributions R.H., X.P.R.-Á., M.M.-T. and J.M.B.d.C. performed the conceptualization. R.H and X.P.R.-Á. edited and coordinated the manuscript and the fieldwork of Sima del Elefante. J.V. contributed to geology, sedimentology and micromorphology. J.M.B.d.C., M.M.-T., M.L., E.S. and L.M.-F. contributed to palaeoanthropology. E.S. and L.M.-F. contributed to virtual reconstruction. E.M.-R. contributed to preservation and conservation. X.P.R.-Á., M.T.-B., A.O., A.d.L.-H., A.B., M.M and E.C. contributed to stone tool technology. R.H., P.S., I.C., A.R.-H., J.M. and A.P. contributed to zooarchaeology and taphonomy. J.M.L.-G., C.N.-L., J.G., H.-A.B. and J.v.d.M. contributed to palaeontology. I.E. and E.A. contributed to archaeobotany. J.M.P. contributed to geochronology. D.L. and A.M. provided comparative samples. E.C., J.M.B.d.C. and J.L.A. directed the excavations.

Competing interests The authors declare no competing interests.

Additional information
Supplementary information The online version contains supplementary material available at https://doi.org/10.1038/s41586-025-08681-0.
Correspondence and requests for materials should be addressed to Rosa Huguet, Xosé Pedro Rodríguez-Álvarez or José María Bermúdez de Castro.
Peer review information *Nature* thanks G. Philip Rightmire, Amélie Vialet and the other, anonymous, reviewer(s) for their contribution to the peer review of this work.

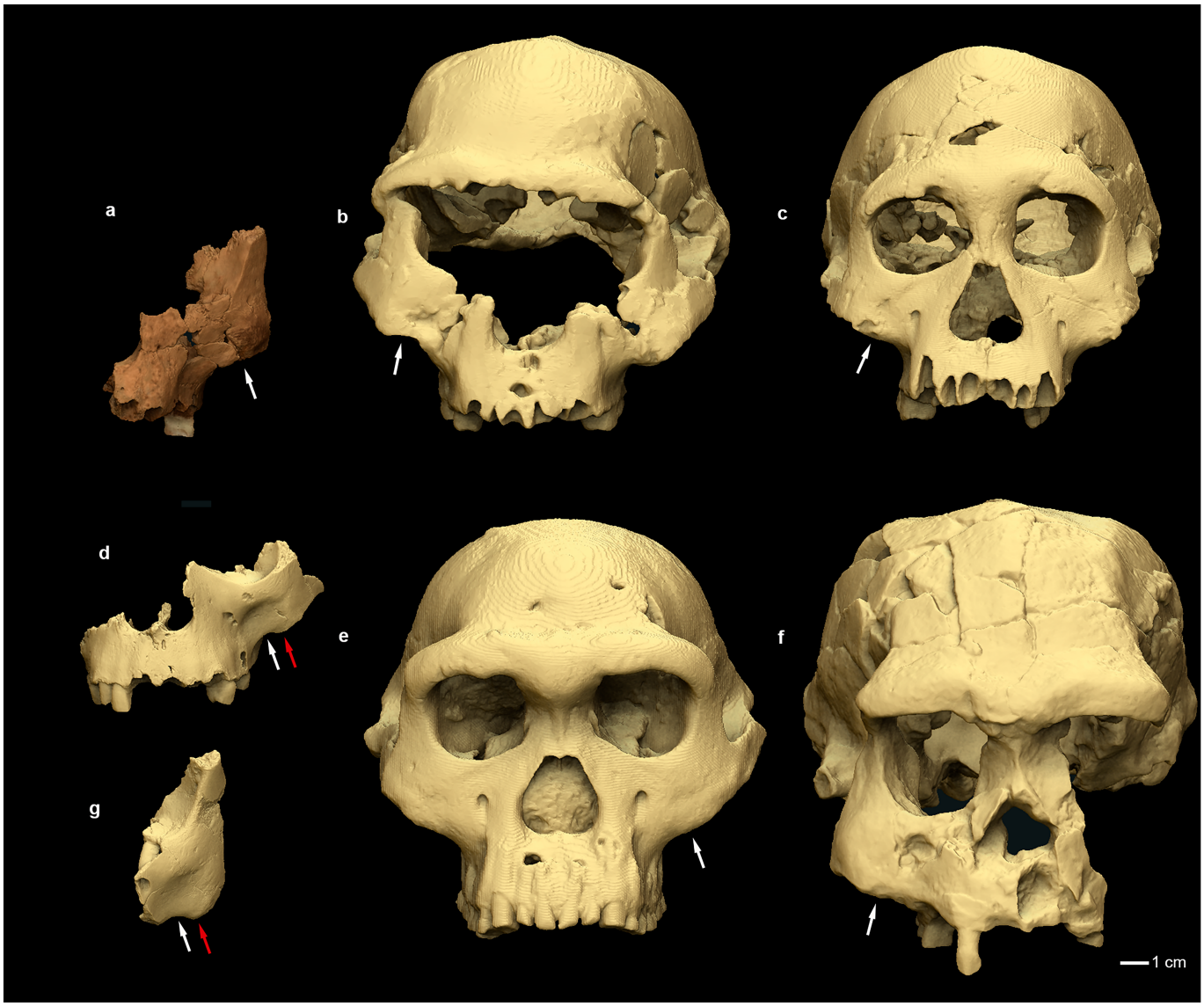

Extended Data Fig. 1 | Comparison of the zygomaxillary border and the zygomaxillary tubercle. Frontal view of the virtual reconstruction of a) ATE7-1, b) D2282, c) D2700, d) ATD6–69, e) D4500, f) Sangiran 17 and g) ATD6–58. White arrow points to the zygomaxillary border which is curved in *H. antecessor* (d,g) and straight in the rest of the specimens, including ATE7-1. Red arrow points to the presence of a zygomaxillary tubercle in ATD6–69 and ATD6-58, a feature that seems to be absent in ATE7–1 and in the Early Pleistocene specimens from Dmanisi and Sangiran portrayed for comparison.

Extended Data Fig. 2 | Comparison of the slope of the infraorbital plate and the lateral nasal margin. Lateral view of the virtual reconstruction of a) ATE7–1, b) D2282, c) KNM-ER-3733, d) ATD6-69, e) D4500 and f) Sangiran 17. The lateral nasal margin of *H. antecessor* is curved, whereas this profile is straight in the rest of the specimens (dashed line 1). The infraorbital plate slopes in an anterior-inferior direction except in ATD6-69, where this surface slopes slightly backwards (dashed line 2).

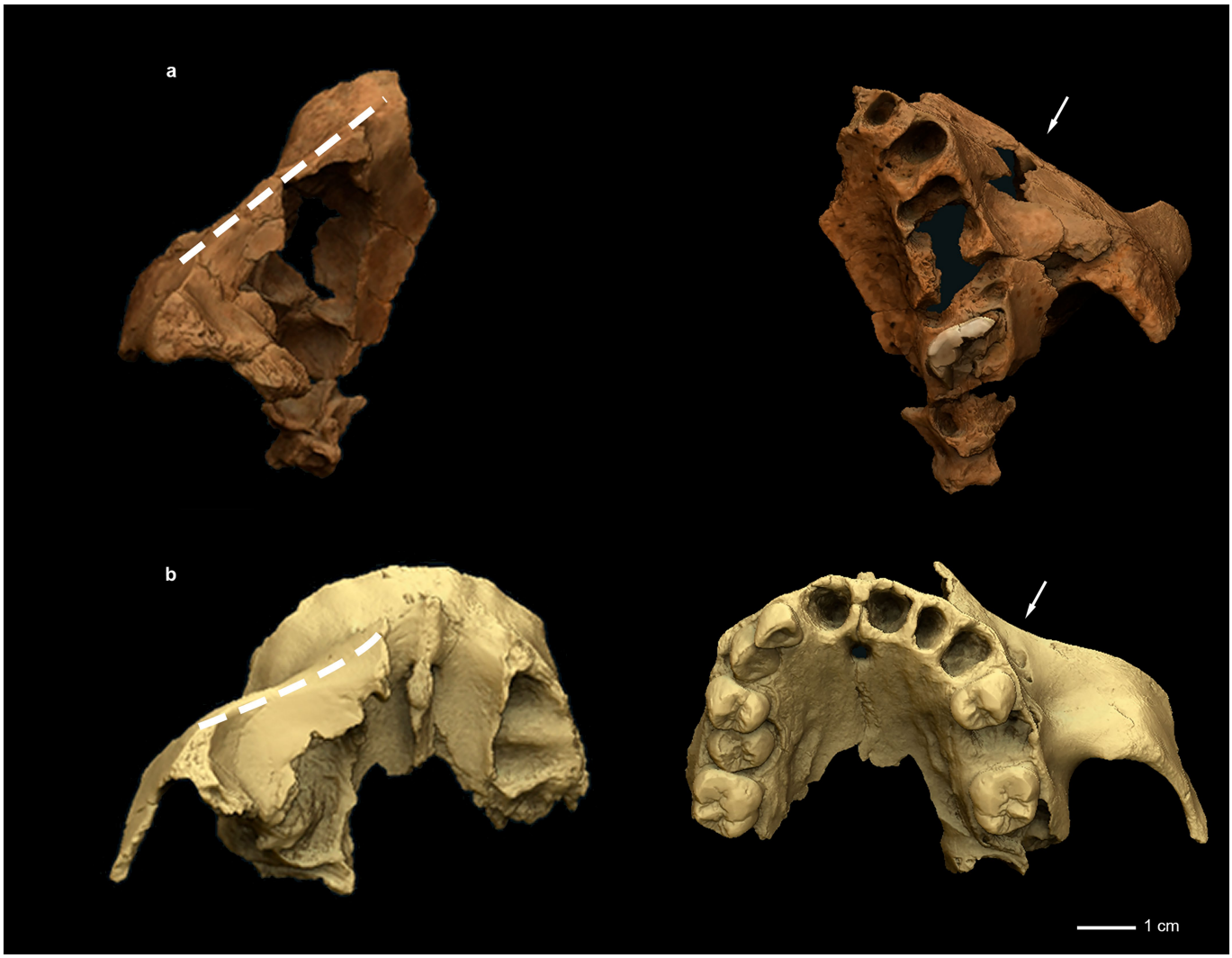

Extended Data Fig. 3 | Comparison of the maxillary flexion. Virtual reconstruction of ATE7–1 and ATD6-69. a) ATE7–1 superior (left) and inferior (right) view, b) ATD6-69 superior (left) and inferior (right). The arrows and the dash lines indicate the differences in the maxillary flexion between both fossils. Whereas the flexion is present in ATD6-69, this feature is absent in ATE7-1.

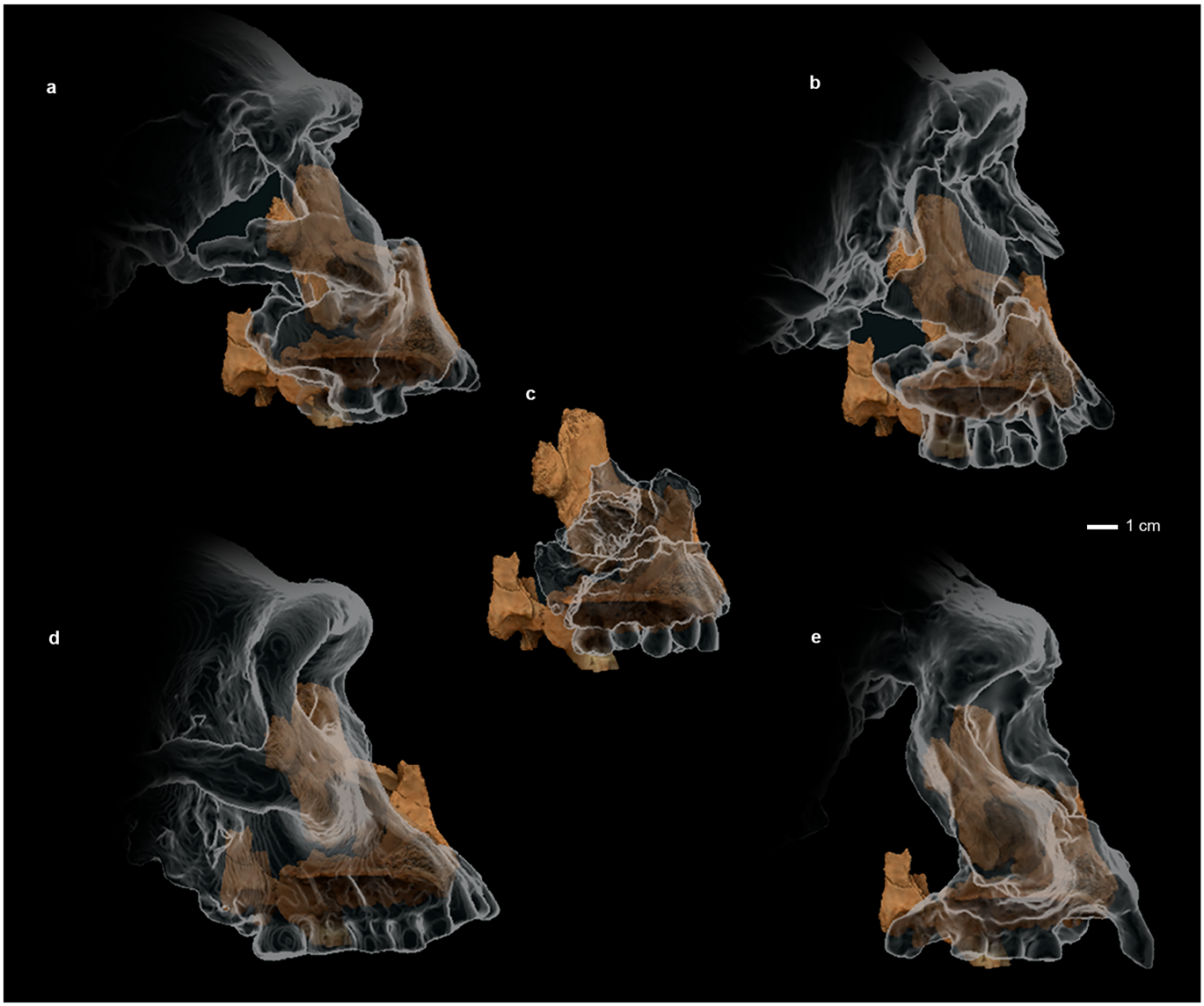

Extended Data Fig. 4 | General comparison of ATE7-1 with Early Pleistocene specimens from Africa and Eurasia in lateral view. Lateral view of the superimposition of the virtual reconstruction of ATE7-1 with a) D2282, b) KNM-ER-3733, c) ATD6-69, d) D4500 and e) Sangiran 17. The comparative fossils are in ghost texture while ATE7 is shown in opaque texture. In this figure it is possible to observe that ATE7-1 shares the same rectilinear morphology of the nasal lateral margin as the comparative specimens except for ATD6-69, which has a curved profile. The morphological differences are also obvious with D4500 because of the long and strongly sloped clivus in the Dmanisi specimen versus the shorter and relatively less inclined clivus in ATE7-1.

Extended Data Fig. 5 | Comparison of the nasal lateral margin in ATE7-1 and ATD6-69. Lateral view of the superimposition of the virtual reconstruction of ATE7-1 (opaque texture) and ATD6-69 (ghost texture). The superimposition highlights the straight course of the nasal lateral margin in ATE7-1 versus the more curved trajectory in ATD6-69.

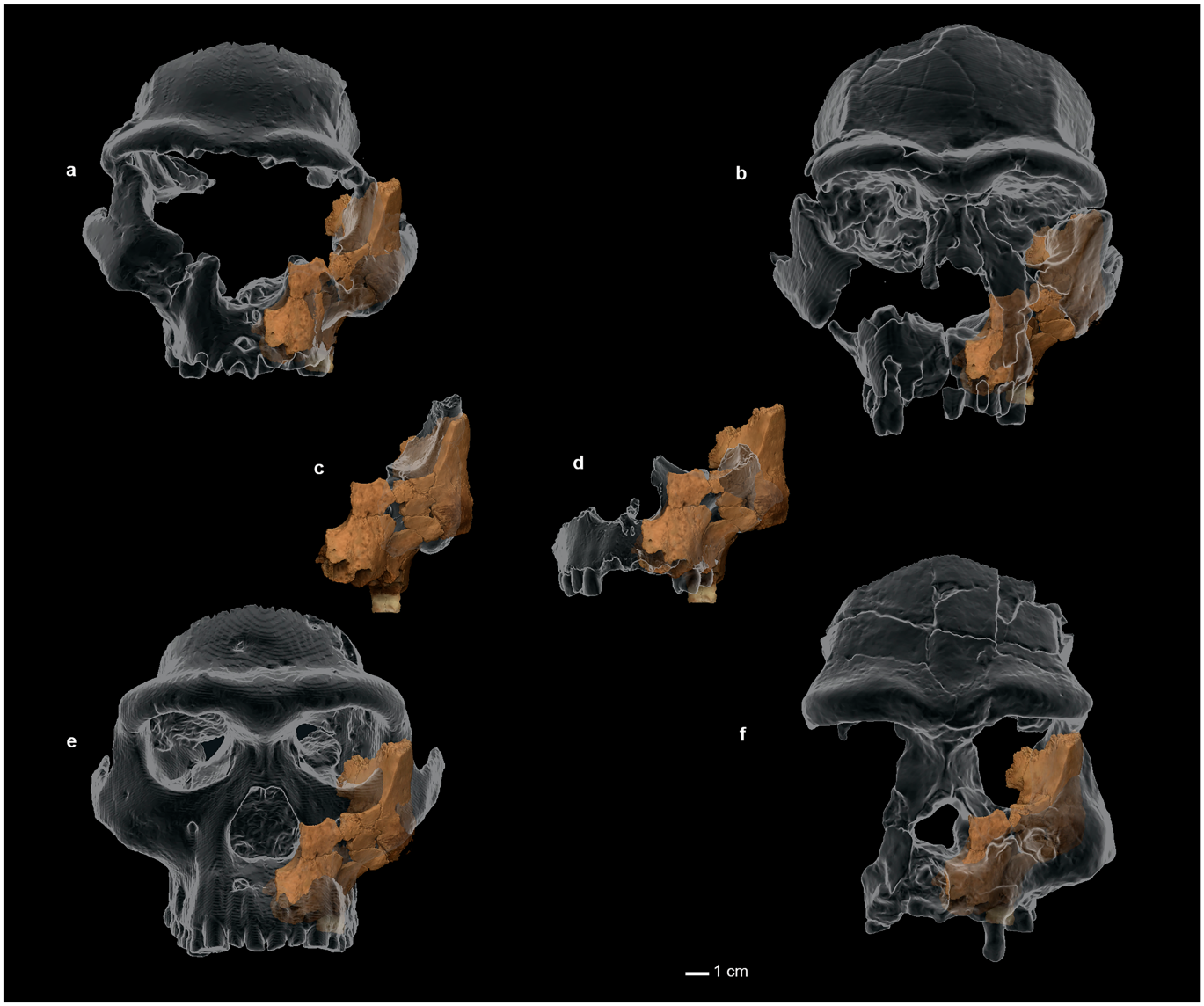

Extended Data Fig. 6 | General comparison of ATE7-1 with Early Pleistocene specimens from Africa and Eurasia in frontal view. Frontal view of the superimposition of the virtual reconstruction of ATE7-1 with a) D2282, b) KNM-ER-3733, c) ATD6-58, d) ATD6-69, e) D4500 and f) Sangiran 17 (mirror reconstruction). The comparative fossils are in ghost texture while ATE7-1 is shown in opaque texture. The comparison highlights the larger facial width of the Early Pleistocene fossils from Africa and Asia due to the anterior projection of their zygomatic bone in comparison to the narrower midface of ATE7-1. Note that the comparison with d) may be influenced by the immature state of this individual.

nature portfolio

Corresponding author(s): Rosa Huguet, X.P. Rodríguez-Àlvarez, J.M. Bermúdez de Castro

Last updated by author(s): 05/12/2024

Reporting Summary

Nature Portfolio wishes to improve the reproducibility of the work that we publish. This form provides structure for consistency and transparency in reporting. For further information on Nature Portfolio policies, see our Editorial Policies and the Editorial Policy Checklist.

Please do not complete any field with "not applicable" or n/a. Refer to the help text for what text to use if an item is not relevant to your study.
For final submission: please carefully check your responses for accuracy; you will not be able to make changes later.

Statistics

For all statistical analyses, confirm that the following items are present in the figure legend, table legend, main text, or Methods section.

n/a	Confirmed	
☐	☒	The exact sample size (*n*) for each experimental group/condition, given as a discrete number and unit of measurement
☐	☒	A statement on whether measurements were taken from distinct samples or whether the same sample was measured repeatedly
☒	☐	The statistical test(s) used AND whether they are one- or two-sided *Only common tests should be described solely by name; describe more complex techniques in the Methods section.*
☒	☐	A description of all covariates tested
☒	☐	A description of any assumptions or corrections, such as tests of normality and adjustment for multiple comparisons
☒	☐	A full description of the statistical parameters including central tendency (e.g. means) or other basic estimates (e.g. regression coefficient) AND variation (e.g. standard deviation) or associated estimates of uncertainty (e.g. confidence intervals)
☒	☐	For null hypothesis testing, the test statistic (e.g. *F*, *t*, *r*) with confidence intervals, effect sizes, degrees of freedom and *P* value noted *Give P values as exact values whenever suitable.*
☒	☐	For Bayesian analysis, information on the choice of priors and Markov chain Monte Carlo settings
☒	☐	For hierarchical and complex designs, identification of the appropriate level for tests and full reporting of outcomes
☒	☐	Estimates of effect sizes (e.g. Cohen's *d*, Pearson's *r*), indicating how they were calculated

Our web collection on statistics for biologists contains articles on many of the points above.

Software and code

Policy information about availability of computer code

Data collection

Data analysis

For manuscripts utilizing custom algorithms or software that are central to the research but not yet described in published literature, software must be made available to editors and reviewers. We strongly encourage code deposition in a community repository (e.g. GitHub). See the Nature Portfolio guidelines for submitting code & software for further information.

Data

Policy information about availability of data

All manuscripts must include a data availability statement. This statement should provide the following information, where applicable:

- Accession codes, unique identifiers, or web links for publicly available datasets
- A description of any restrictions on data availability
- For clinical datasets or third party data, please ensure that the statement adheres to our policy

Research involving human participants, their data, or biological material

Policy information about studies with human participants or human data. See also policy information about sex, gender (identity/presentation), and sexual orientation and race, ethnicity and racism.

Reporting on sex and gender	
Reporting on race, ethnicity, or other socially relevant groupings	
Population characteristics	
Recruitment	
Ethics oversight	

Note that full information on the approval of the study protocol must also be provided in the manuscript.

Field-specific reporting

Please select the one below that is the best fit for your research. If you are not sure, read the appropriate sections before making your selection.

☐ Life sciences ☐ Behavioural & social sciences ☒ Ecological, evolutionary & environmental sciences

For a reference copy of the document with all sections, see nature.com/documents/nr-reporting-summary-flat.pdf

Life sciences study design

All studies must disclose on these points even when the disclosure is negative.

Sample size	
Data exclusions	
Replication	
Randomization	
Blinding	

Behavioural & social sciences study design

All studies must disclose on these points even when the disclosure is negative.

Study description	
Research sample	
Sampling strategy	
Data collection	
Timing	
Data exclusions	
Non-participation	
Randomization	

Ecological, evolutionary & environmental sciences study design

All studies must disclose on these points even when the disclosure is negative.

Study description	- The study had implied the analysis of a midface hominin fossil at the TE7 level of the Sima del Elefante site in Atapuerca, dated within a range of 1.1 to 1.5 million years ago.The fossil representing the earliest known facial remains in Western Europe.
Research sample	- We have analysed a hominin remain ATE7-1 recovered at Sima del Elefante site,hosted at IPHES (Tarragona, Spain), and its archaeological and palaeoecological context.
Sampling strategy	- The fossil was recovered from level 7 during the 2022 excavation season and subsequent conservation and preservation treatments were carried out.
Data collection	- The morphology of the face and the teeth are described based on the analysis of the original 351 fossils and/or virtual reconstruction after micro-computed tomographic (microCT) scanning.
Timing and spatial scale	- The study of this material has been carried out between 2022-2024.
Data exclusions	- In this study we have not excluded any relevant data.
Reproducibility	- The analyses carried out in this work are reproducible.
Randomization	- We have not used any kind of radomisation test.
Blinding	- It is not relevant to this study

Did the study involve field work? [X] Yes [ ] No

Field work, collection and transport

Field conditions	The fieldwork was carried out during the summer of 2022 with good conditions for all participating members.
Location	Sima del Elefante site (Sierra de Atapuerca, Spain, Western of Europe.
Access & import/export	The access of sample has been easy, it has not been necessary to export or import material.
Disturbance	In this study there has been no disturbance

Reporting for specific materials, systems and methods

We require information from authors about some types of materials, experimental systems and methods used in many studies. Here, indicate whether each material, system or method listed is relevant to your study. If you are not sure if a list item applies to your research, read the appropriate section before selecting a response.

Materials & experimental systems

n/a	Involved in the study
[X]	[ ] Antibodies
[X]	[ ] Eukaryotic cell lines
[ ]	[X] Palaeontology and archaeology
[X]	[ ] Animals and other organisms
[X]	[ ] Clinical data
[X]	[ ] Dual use research of concern
[X]	[ ] Plants

Methods

n/a	Involved in the study
[X]	[ ] ChIP-seq
[X]	[ ] Flow cytometry
[X]	[ ] MRI-based neuroimaging

Antibodies

Antibodies used	
Validation	

Eukaryotic cell lines

Policy information about cell lines and Sex and Gender in Research

Cell line source(s)	
Authentication	
Mycoplasma contamination	
Commonly misidentified lines (See ICLAC register)	

Palaeontology and Archaeology

Specimen provenance	Specimens provence from Sima del Elefante site (Atapuerca, Spain).
Specimen deposition	Specimen hosted at IPHES (Tarragona, Spain).
Dating methods	From radiometric and biochronological data published by Carbonell et al. 2008 in Nature. The numerical data was obtained for the above level TE9c (1.2 ± 0.16 Ma) is based on a combination of paleomagnetism, cosmogenic nuclides and biostratigraphy to around 1.2 Ma.

☐ Tick this box to confirm that the raw and calibrated dates are available in the paper or in Supplementary Information.

Ethics oversight	

Note that full information on the approval of the study protocol must also be provided in the manuscript.

Animals and other research organisms

Policy information about studies involving animals; ARRIVE guidelines recommended for reporting animal research, and Sex and Gender in Research

Laboratory animals	
Wild animals	
Reporting on sex	
Field-collected samples	
Ethics oversight	

Note that full information on the approval of the study protocol must also be provided in the manuscript.

Clinical data

Policy information about clinical studies

All manuscripts should comply with the ICMJE guidelines for publication of clinical research and a completed CONSORT checklist must be included with all submissions.

Clinical trial registration	
Study protocol	
Data collection	
Outcomes	

Dual use research of concern

Policy information about dual use research of concern

Hazards

Could the accidental, deliberate or reckless misuse of agents or technologies generated in the work, or the application of information presented in the manuscript, pose a threat to:

No	Yes	
☐	☐	Public health
☐	☐	National security
☐	☐	Crops and/or livestock
☐	☐	Ecosystems
☐	☐	Any other significant area

Experiments of concern

Does the work involve any of these experiments of concern:

No	Yes	
☐	☐	Demonstrate how to render a vaccine ineffective
☐	☐	Confer resistance to therapeutically useful antibiotics or antiviral agents
☐	☐	Enhance the virulence of a pathogen or render a nonpathogen virulent
☐	☐	Increase transmissibility of a pathogen
☐	☐	Alter the host range of a pathogen
☐	☐	Enable evasion of diagnostic/detection modalities
☐	☐	Enable the weaponization of a biological agent or toxin
☐	☐	Any other potentially harmful combination of experiments and agents

Plants

Seed stocks

Novel plant genotypes

Authentication

ChIP-seq

Data deposition

☐ Confirm that both raw and final processed data have been deposited in a public database such as GEO.

☐ Confirm that you have deposited or provided access to graph files (e.g. BED files) for the called peaks.

Data access links
May remain private before publication.

Files in database submission

Genome browser session
(e.g. UCSC)

Methodology

Replicates

Sequencing depth

Antibodies

Peak calling parameters

Data quality

Software

Flow Cytometry

Plots

Confirm that:

☐ The axis labels state the marker and fluorochrome used (e.g. CD4-FITC).

☐ The axis scales are clearly visible. Include numbers along axes only for bottom left plot of group (a 'group' is an analysis of identical markers).

☐ All plots are contour plots with outliers or pseudocolor plots.

☐ A numerical value for number of cells or percentage (with statistics) is provided.

Methodology

Sample preparation	
Instrument	
Software	
Cell population abundance	
Gating strategy	

☐ Tick this box to confirm that a figure exemplifying the gating strategy is provided in the Supplementary Information.

Magnetic resonance imaging

Experimental design

Design type	
Design specifications	
Behavioral performance measures	

Imaging type(s)	
Field strength	
Sequence & imaging parameters	
Area of acquisition	

Diffusion MRI ☐ Used ☐ Not used

Preprocessing

Preprocessing software	
Normalization	
Normalization template	
Noise and artifact removal	
Volume censoring	

Statistical modeling & inference

Model type and settings	
Effect(s) tested	

Specify type of analysis: ☐ Whole brain ☐ ROI-based ☐ Both

Statistic type for inference

(See Eklund et al. 2016)

Correction

Models & analysis

n/a	Involved in the study
☐	☐ Functional and/or effective connectivity
☐	☐ Graph analysis
☐	☐ Multivariate modeling or predictive analysis

Functional and/or effective connectivity

Graph analysis

Multivariate modeling and predictive analysis